a) Aminoacylation conformation

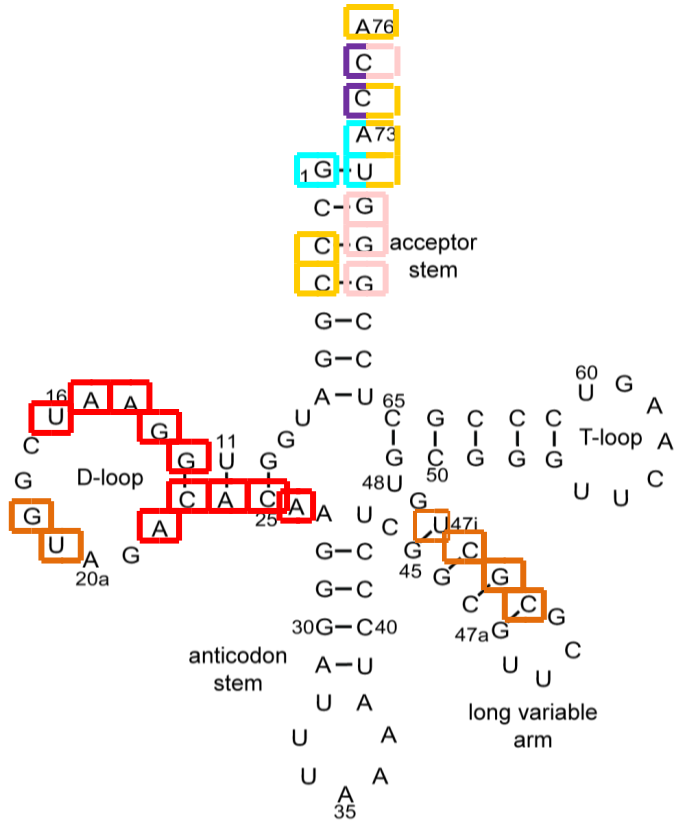

Catalytic
Editing
ZN1
Leucine-specific
Anti-codon
C-terminal

b) Editing conformation

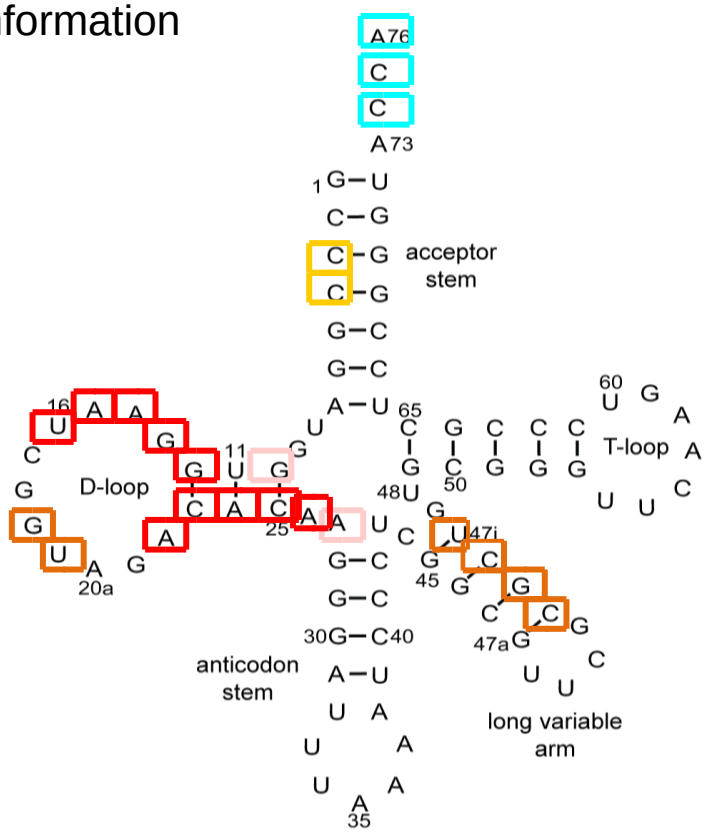

Supplementary Figure 1. Contacts with *E. coli* $tRNA_5^{Leu}$(UAA) in LeuRSEC-tRNA functional complexes. (a) Nucleotides that interact with LeuRS in the aminoacylation state and **(b)** in the editing state are indicated by boxes using the domain color code introduced in Figure 1.

c) Electron density of the 3´ end tRNA-LeuAMS

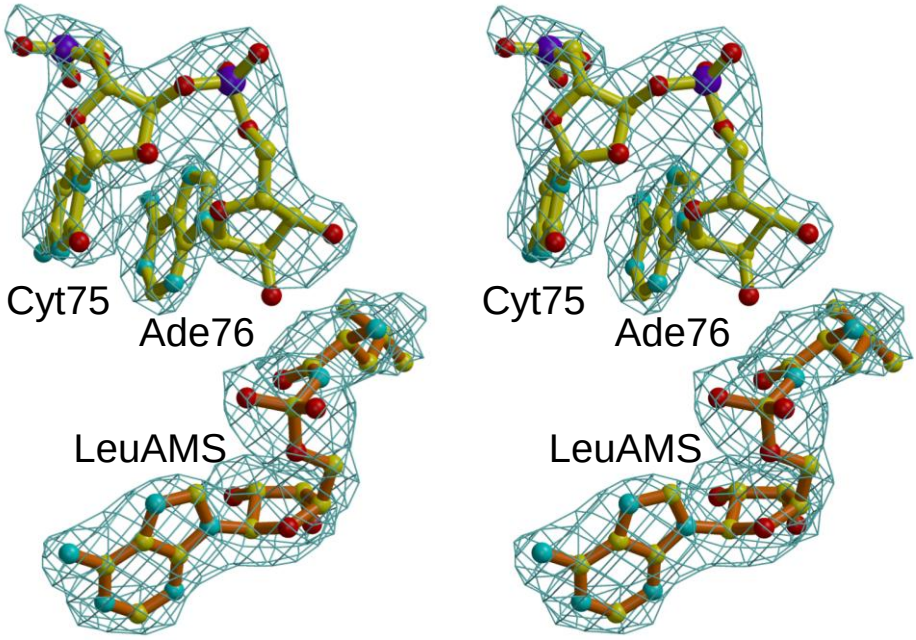

d) 3′ end tRNA in bacterial and archaeal LeuRS

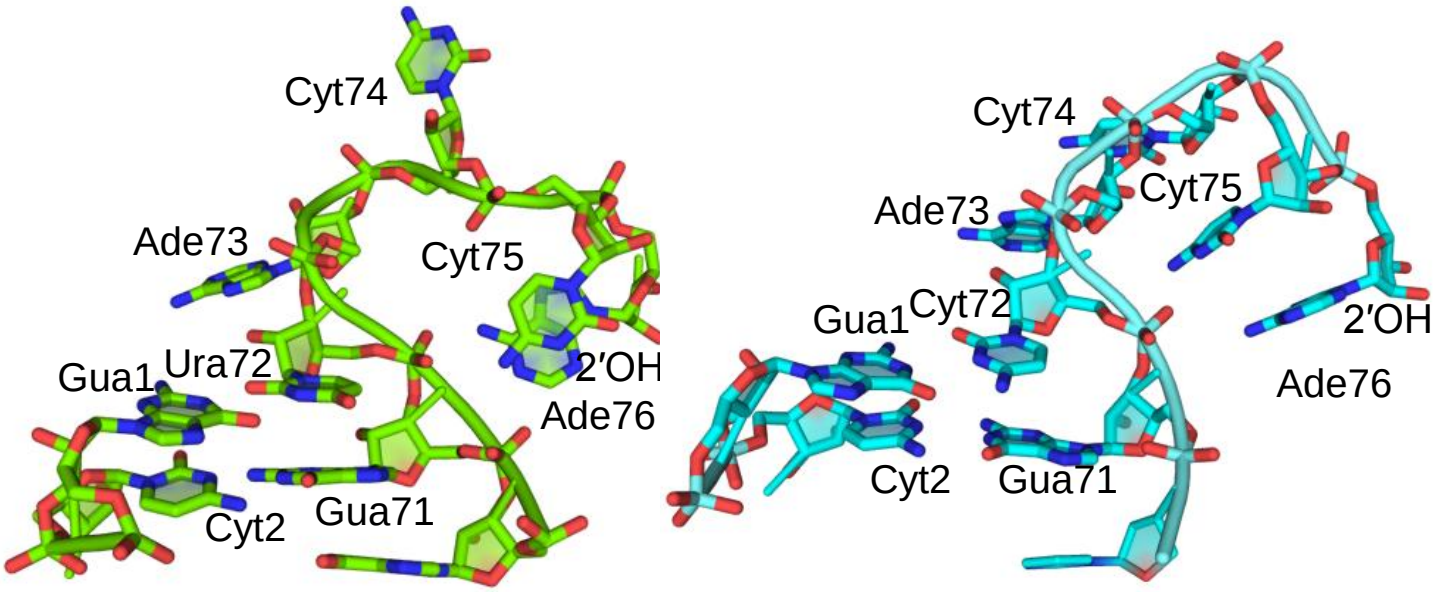

Supplementary Figure 1(c) Stereo diagram showing unbiased m(Fo-Fc) difference electron density (contoured at 3σ) for bases Cyt75 and Ade76 of the tRNA and LeuAMS in the *E. coli* aminoacylation complex. The density was obtained by rebuilding and refinement of the molecular replacement model without inclusion of 75-Cyt-Ade-76 and LeuAMS. **(d)** The tRNA 3′ end conformation in the aminoacylation states of LeuRSEC (left, this work) and LeuRSPH (right, PDB 1WZ2) after superposition of the bodies of the enzymes.

Supplementary Figure 2 Phylogenetic analysis of bacterial LeuRS.

a)

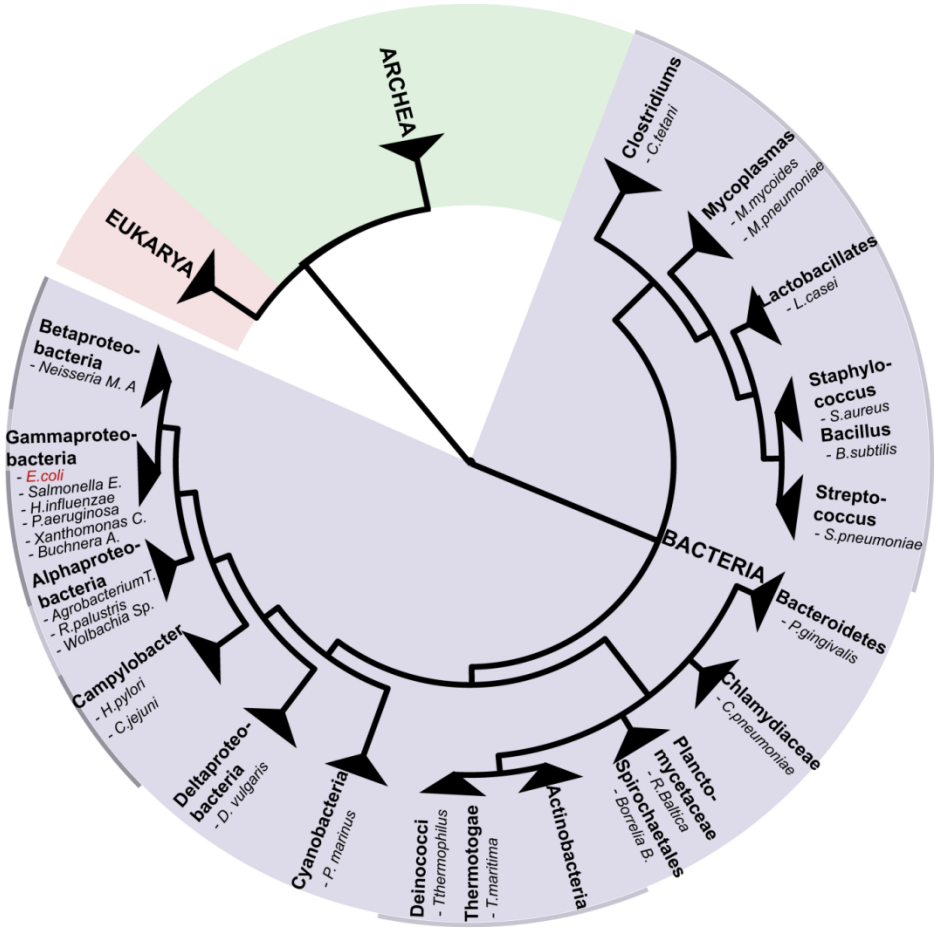

b-e) Sequence alignment of bacterial LeuRS

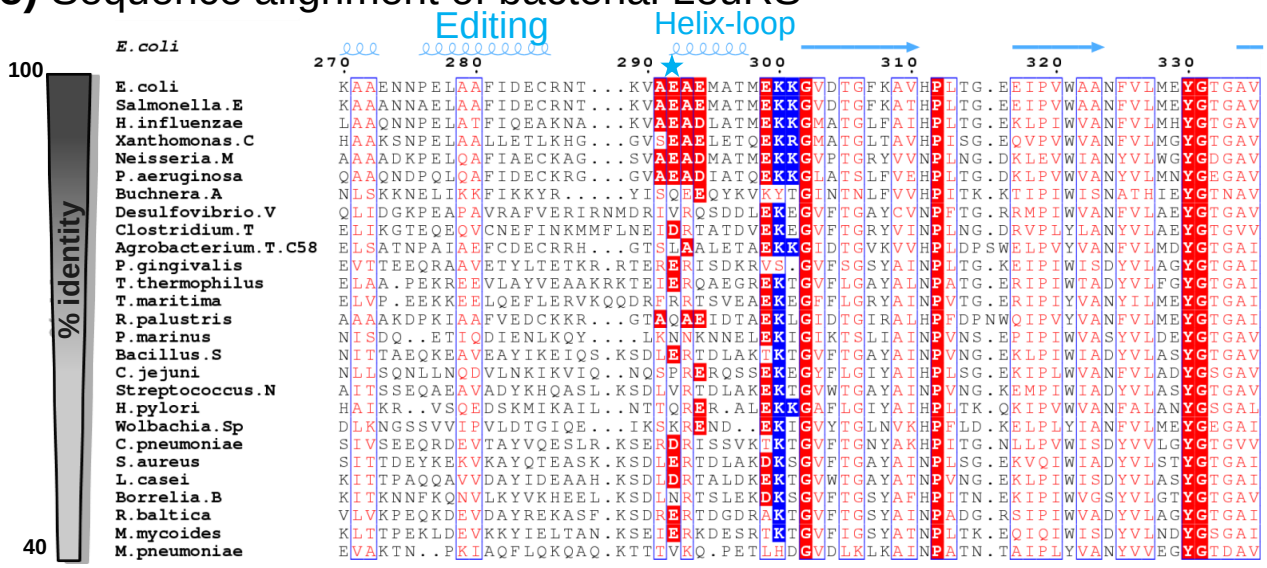

Supplementary Figure 2. Phylogenetic analysis of bacterial LeuRS. (a) Circular phylogenetic tree showing the main bacterial clades (in bold letters) and subclades in the prokaryotic kingdom. Representative members for each bacterial subclade (in regular letters) were used for the sequence alignments in **b-e)**. Sequences for each species are ordered from top to down according to the identity to *E. coli* LeuRS, and the corresponding secondary structure elements in *E. coli* LeuRS are coloured as in Figure 1. Some of the key residues for aminoacylation/proof-reading and for tRNA recognition are highlighted by stars.

c) Sequence alignment of bacterial LeuRS

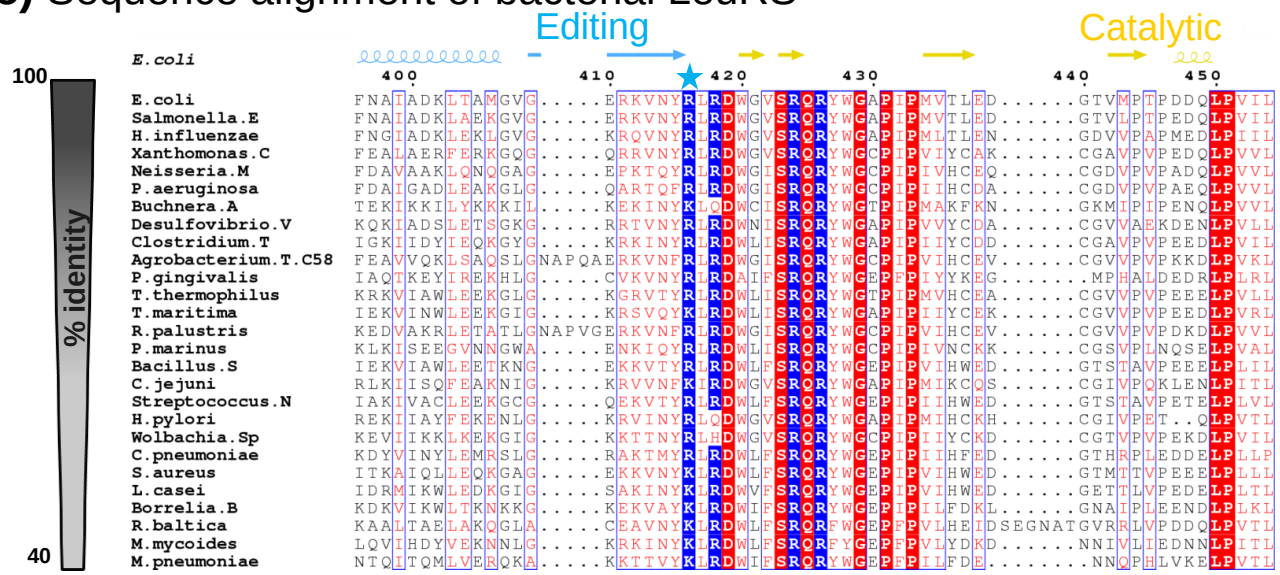

d)

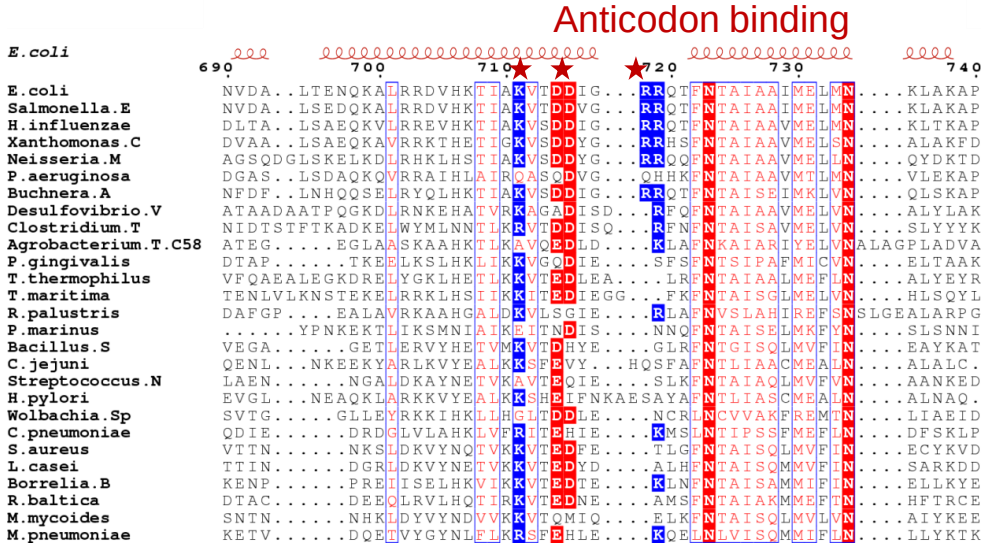

e)

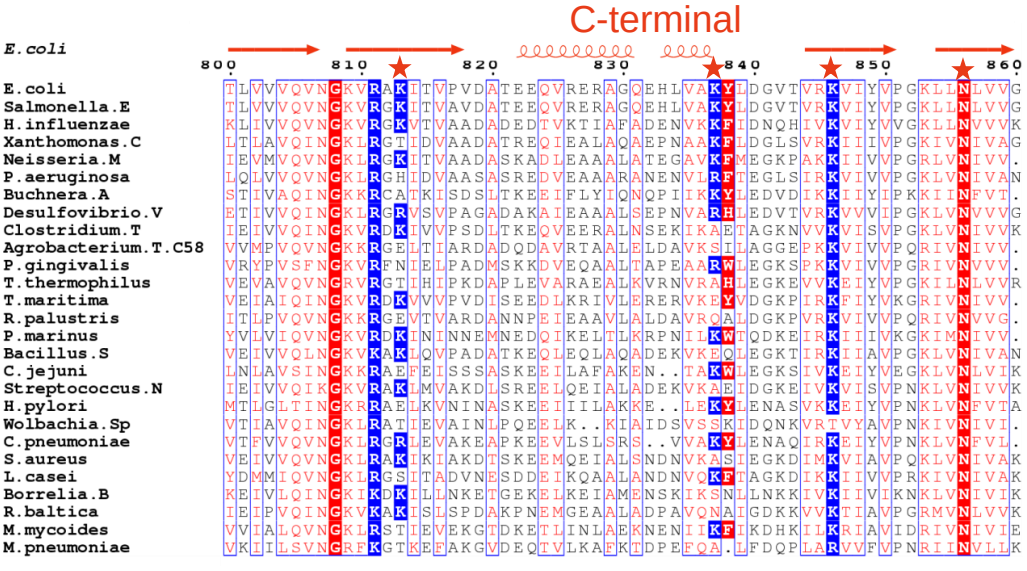

Supplementary Figure 3. Comparison of LeuRSEC and LeuRSTT.

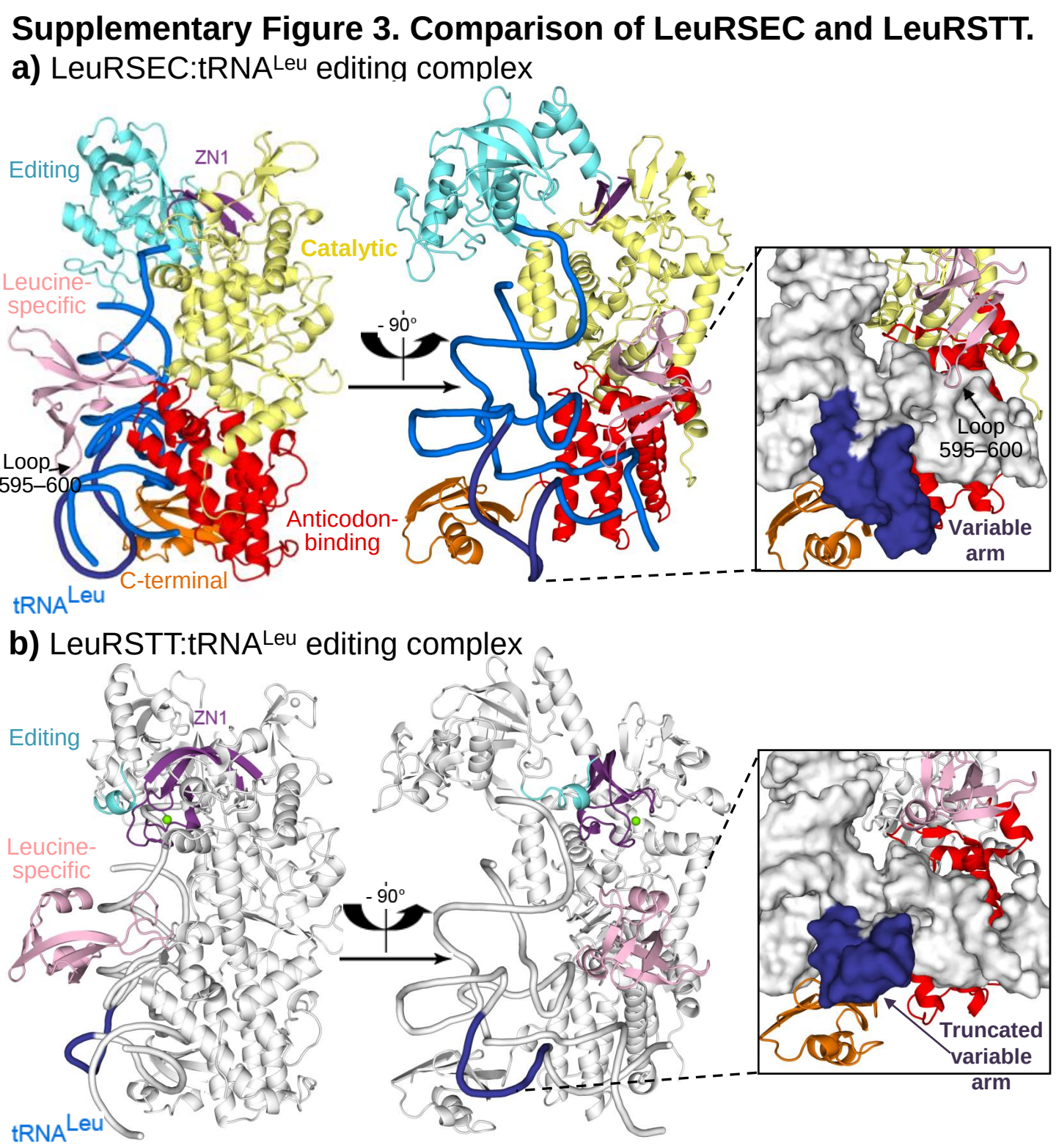

Supplementary Figure 3. Comparison between (a) *E. coli* and (b) *T. thermophilus* LeuRS:tRNA^{Leu} editing complexes. For each complex, two orientations with a rotation about the vertical axis by 90° clockwise are shown. Domains are colour coded as in Figure 1. The main differences between the two complexes are highlighted on the *T. thermophilus* editing complex. The inset panels show tRNA^{Leu} shape recognition by the two LeuRSs. tRNA^{Leu} (grey surface) is grasped between the anticodon-binding (red) and the C-terminal (orange) domains. The loop 595-600 in the leucine-specific domain (pink) and specific bases of the variable arm of the tRNA (blue surface) participate in the interactions in the *E. coli* complex, but not in the *T. thermophilus* complex.

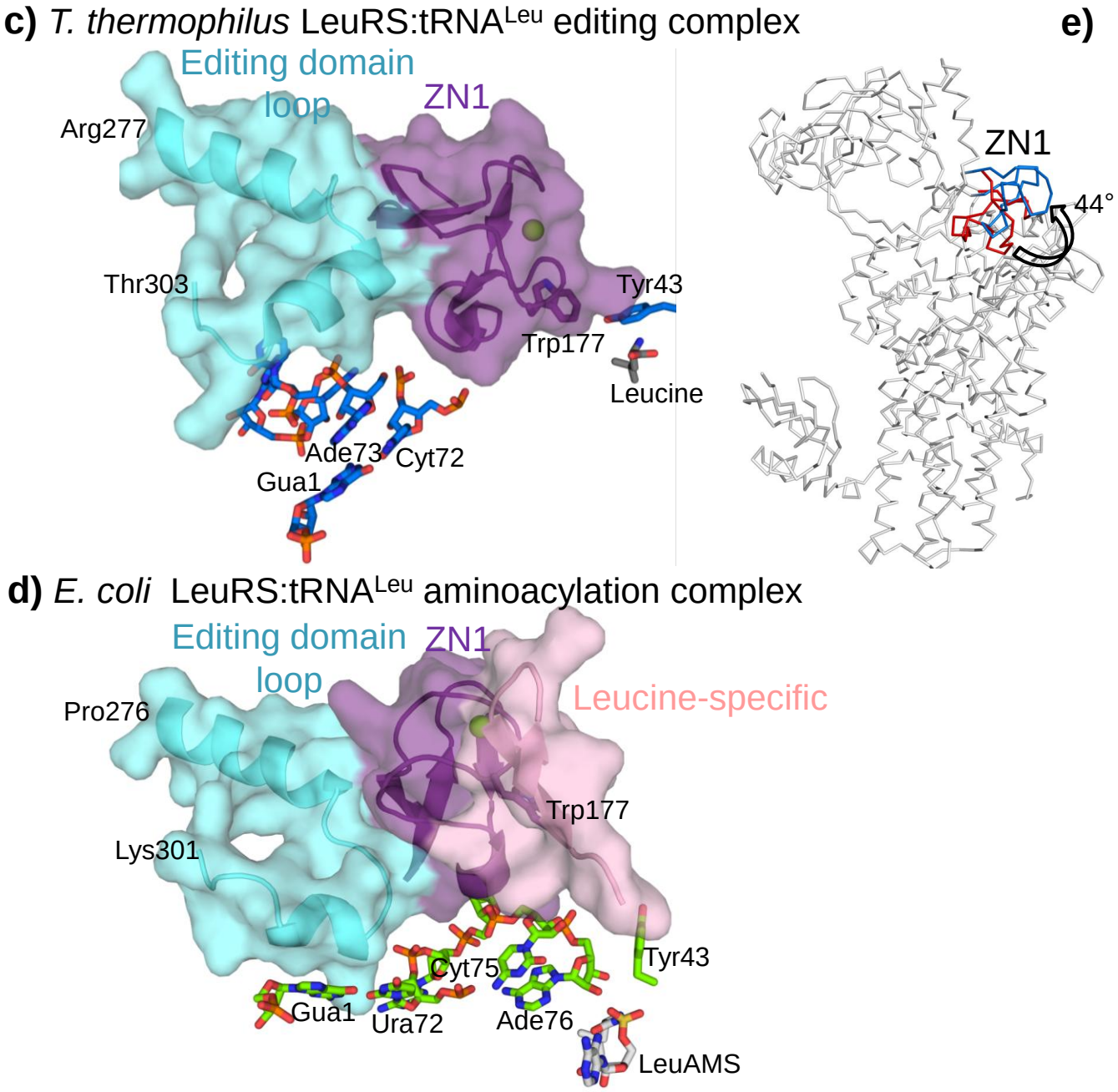

Supplementary Figure 3c-e. Comparison between the ZN1 domain orientation and interface with the editing domain in the (c) *T. thermophilus* LeuRS:tRNA^{Leu} editing complex and (d) *E. coli* LeuRS:tRNA^{Leu} aminoacylation complex. Different interactions with the editing domain loop 277-303 stabilise the ZN1 domain in the closed/down position **(c)** in the LeuRSTT editing complex or in the open/up position **(d)** in the LeuRSEC aminoacylation state. Both figures are drawn with the same view after superposition of the enzyme bodies The last acceptor stem base-pair and 3′ end of the tRNA is shown. In the closed position **(d)**, the ZN1 domain stabilises the stacking of Tyr43 over the leucine substrate. With the ZN1 domain in this position, binding of the 3′ end of the tRNA in the functional aminoacylation configuration is impossible. The closed configuration has not so far been observed in the *E. coli* system where the ZN1 domain is disordered, presumably due to flexibility in the LeuRSEC editing complex and there is no LeuRSEC structure in the absence of tRNA. (**e).** Schematic view of the rotation of the flexibly linked ZN1 domain between the editing (red) and aminoacylation states (blue), after superposition of the enzyme bodies (*E .coli* LeuRS is represented in grey). The rotation to the open position allows 3′ end binding for aminoacylation.

Supplementary Figure 4. Mutational analysis of LeuRSEC.

a)

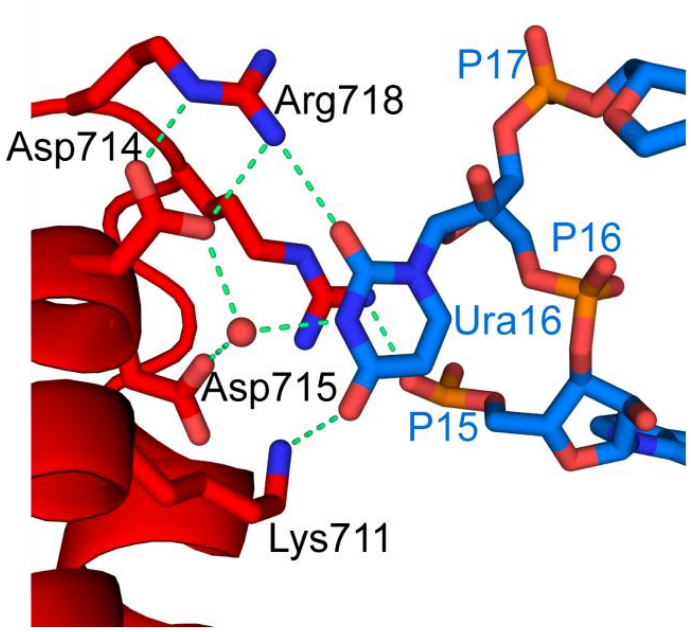

b)

Anticodon-binding mutations

	K_mtRNA (mM)	K_{cat} (s^{-1})	K_{cat} / K_m (s^{-1} mM^{-1})	Relative
WT	1.5	2.4	1.6	1
D714A	2.9	3.6	1.4	0.87
D715A	2.2	1.0	0.4	0.25
R718A	6.0	2.5	0.4	0.25
Triple	18.1	1.7	0.1	0.06

tRNA^{Leu} (UAA) mutations

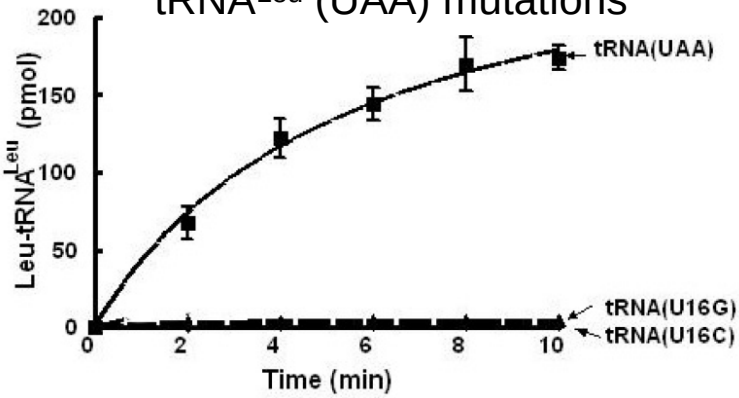

Supplementary Figure 4a,b. Ura16 is a new tRNA identity element in *E. coli*. (a) Specific recognition of Ura16 by LeuRSEC as observed in both the editing and aminoacylation LeuRS:tRNA^{Leu} complexes. The residues of the anticodon-binding domain (red) involved in the recognition of Ura16 are shown as sticks. **(b)** Effects of anticodon-binding domain mutations (left) on the kinetic parameters of LeuRSEC and effects of Ura16 mutations (right) on the aminoacylation of tRNA^{Leu}. Error bars represent standard deviations for three independent reactions.

c) Arrhenius plots

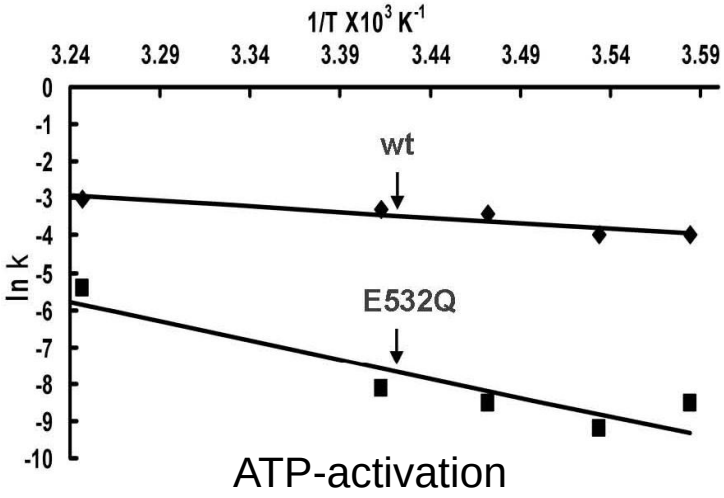

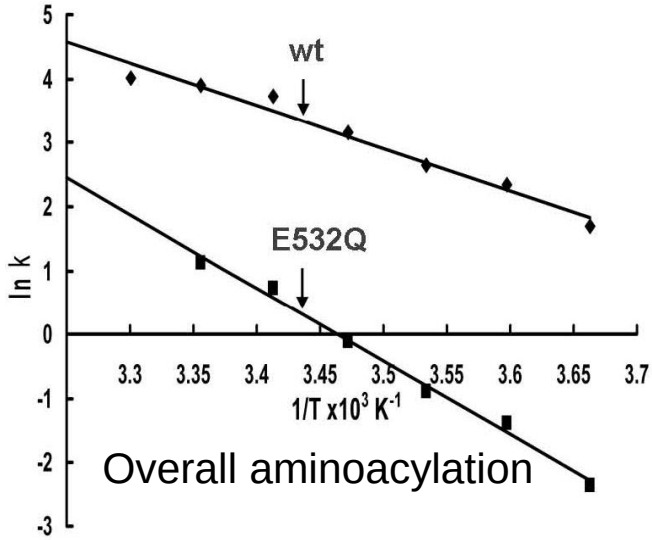

d) Schematic free energy diagrams

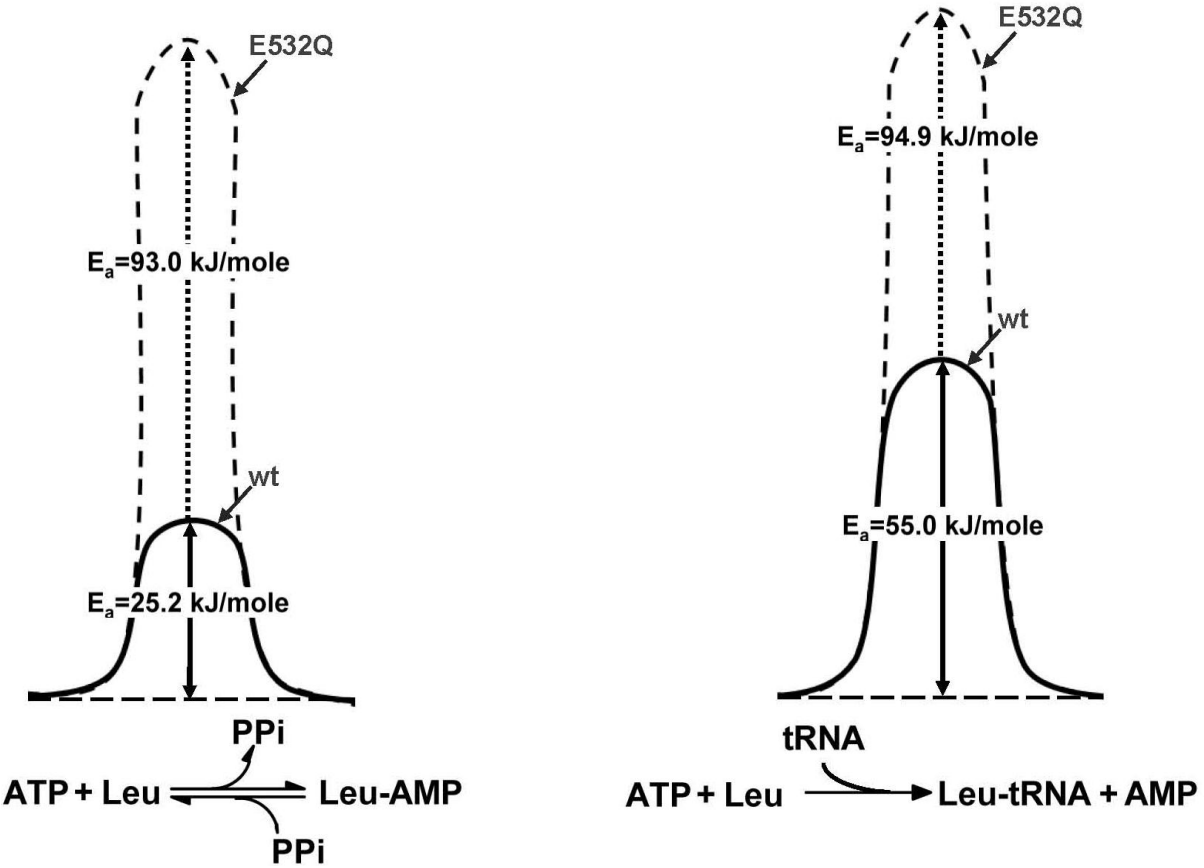

Supplementary Figure 4c,d. Glu532 is involved in ATP-activation. (c) Arrhenius plots showing the leucine-dependent PPi-ATP exchange activity (left) and overall aminoacylation (right) measured at 20, 25, 30, 35 and 40 ^{0}C for the wild-type (diamonds) and the E532Q mutant (squares). **(d)** Free energy diagrams representing the ATP-activation energies (left) and overall aminoacylation energies (right) for the wild type (continuous line) and the mutant E532Q (dashed line) *Ec*LeuRS.

Supplementary Table 1 Buried surface area due to tRNA binding

Buried surface (Å²)[a]

	E. coli aminoacylation	*E. coli* editing	*T. thermophilus* editing
Total	5 759	4 830	4 144
Catalytic	1 867	559	610
ZN1	456	-	110
Editing	416	1 065	1 210
Leucine-specific (including KMSKS)	433	368	0
Anticodon-binding	1 716	1 760	1 390
C-terminal	1 171	1 151	894

[a]Surfaces were calculated using NACCESS (http://www.bioinf.manchester.ac.uk/naccess/). Accessible surface area buried upon complex formation (S) was obtained using the formula: $S = S_{prot} + S_{tRNA} - S_{complex}$.

Buried surface normalized

	E. coli aminoacylation	*E. coli* editing	*T. thermophilus* editing
Total	1	1	1
Catalytic	0.3	0.114	0.144
ZN1	0.075	-	0.026
Editing	0.068	0.217	0.287
Leucine-specific (including KMSKS)	0.071	0.075	0
Anticodon-binding	0.283	0.359	0.33
C-terminal	0.193	0.234	0.212

Domains limits

	E. coli	*T. thermophilus*
Catalytic	1-148 194-224 416-568	1-148 195-223 148-576
ZN1	149-193	149-194
Editing	225-415	224-417
Leucine-specific (including KMSKS)	569-629	577-646
Anticodon-binding	630-795	647-812
C-terminal	796-860	813-878